



**HAL**  
open science

## **DISTRIBUTION OF MEAN SPATIAL RAINFALL IN THE CHARI-LOGONE BASIN FROM 1960-2015**

Abdallah Mahamat Nour, Christine Vallet-Coulomb, Siddig Ahmed Abbas

► **To cite this version:**

Abdallah Mahamat Nour, Christine Vallet-Coulomb, Siddig Ahmed Abbas. DISTRIBUTION OF MEAN SPATIAL RAINFALL IN THE CHARI-LOGONE BASIN FROM 1960-2015. International Journal of Engineering Sciences & Research Technology, In press, 10.5281/zenodo.3542442 . hal-03110974

**HAL Id: hal-03110974**

**<https://hal.science/hal-03110974>**

Submitted on 14 Jan 2021

**HAL** is a multi-disciplinary open access archive for the deposit and dissemination of scientific research documents, whether they are published or not. The documents may come from teaching and research institutions in France or abroad, or from public or private research centers.

L'archive ouverte pluridisciplinaire **HAL**, est destinée au dépôt et à la diffusion de documents scientifiques de niveau recherche, publiés ou non, émanant des établissements d'enseignement et de recherche français ou étrangers, des laboratoires publics ou privés.

## ABSTRACT

The Chari-Logone basin (BCL), which is the focus of this work, is the hydrologically active part of the Lake Chad Basin. It covers an area of 613 000 km<sup>2</sup>, and its banks are surrounded by a series of mountain ranges: Guera, Ouaddaï, Central African Massif and Adamaoua. The climate of the Chari-Logone basin is contrasted, from the tropical climate to the Sahelian climate.

We synthesized, analyzed and exploited all rainfall data available on the Chari-Logone basin during the period 1950-2015 in order to characterize spatial contrasts, temporal variations and sensitivities to climatic variations. These data come from Chad's national services and literature. We used the method of Kriging interpolation with the software R for the spatialization of these data. The interpolation is made on eighty-nine rainfall stations, and the mesh chosen is a regular grid with a pitch of 0.1°. Data analysis showed that the distribution of interannual mean rainfall is mainly along a typical south - north gradient of the Sudano - Sahelian region. The highest values are always recorded at the southwestern extremities corresponding to the direction of entry of the monsoon flow in the basin, with probably a slight orographic effect. Thus, Sudan's wetter regions of the south-west (1600 to 800 mm) are progressively transferred to the Sahelian regions, which are sparsely watered in the north-east (between 800 and 200 mm).

**KEYWORDS:** Chari-Logone, Lake Chad, rainfall, kriging, spatialization.

## 1. INTRODUCTION

The Lake Chad Basin, due to its geographical location in arid and semi-arid zones, suffers from repeated droughts linked to rainfall deficits and resulting in the reduction of surface water bodies and groundwater resources. Recent decades have seen a dramatic increase in the concentration of greenhouse gases in the global atmosphere and substantial changes in African land cover (L. D. Meyer, 1981). These aspects of recent environmental change are suspected of forcing changes in global (Houghton, 1992) and regional (S. E. Nicholson, 2001) climates. Drought control practices need accurate estimates of rainfall in space and time (Joyce & Arkin, 1997, Verdin *et al.*, 2016). The spatio-temporal estimation of precipitation is important for efficient management of natural resources and for mitigating natural risks (Leroux, 1986, Funk *et al.*, 2015). This concept is true in developing regions and regions that are exposed to extreme events (Chevallier & Pouyaud, 1996). Rainfall data are used as an alternative to support early warning of hydro-meteorological systems (Verdin *et al.*, 2016). They are more reliable to the extent that they are directly measured in the field. However, rain gauge observations are often limited in African regions, clustered in cities or populated areas. Data from few gauge stations can provide little information on the spatial extent and intensity of a given precipitation event (Rozante *et al.*, 2010).

In these situations, the data provided by the very few rainfall stations of the General Directorate of National Meteorology of Chad (DGMN) that are functional and available today do not allow us to advance our knowledge of the spatio-temporal structure of rain and hardly allowed to develop models. Satellite-derived precipitation data is an interesting alternative (Huffman *et al.*, 1995), but this data may tend to underestimate the magnitude of wet events because of their dependence on satellite algorithms. recovery and the indirect



relationship between infrared observations by satellite and precipitation intensities (Xie & Arkin, 1997). However, there are annual and monthly rainfall series in the Lake Chad Basin from the 1940s to the 1960s compiled by ORSTOM researchers. Such precipitation data are not representative of the last decades, especially the new period from 1980 to 2010. It is important to set up specific methods to update and support the study of spatio-temporal of the Lake Chad Basin. This will serve as an input parameter to the hydrological model so that precipitation is still considered a key element of watershed studies. So, the method used in this study is kriging interpolation. It should be noted that this method had already taken place in other parts of the world, notably in the United States, Europe and Asia (Woodley *et al.*, 1979, Dingman *et al.*, 1988, Goovaerts, 2000, Subyani, 2004, Baillargeon, 2005).

## 2. STUDY AREA

### 2.1 Lake Chad basin and Chari-Logone system

The Lake Chad Basin (BLT) is located in Central Africa, between 6° and 24° North latitude and 8° and 24° East longitude. It occupies an area of approximately 2 500 000 km<sup>2</sup>, 8% of that of the African continent and is divided between Algeria, Cameroon, Libya, Niger, Nigeria, the Central African Republic, Sudan and Chad. This basin occupies a large basin bordered by Hoggar and Tibesti in the north, the mountain ranges of Ennedi and Ouaddaï in the east, the trays of Jos (Nigeria) and Aïr (Niger) to the west those of Oubangui (Central African Massif) in the south as well as the Adamaoua massif in Cameroon (Fig. 1). This mountainous ensemble shows a variety of reliefs. In the center of the basin, we find the low-contrast reliefs of Kanem and Borkou formed by an alternation of dunes and depressions (Schuster *et al.*, 2005).

The Lake Chad Basin consists mainly of two sub-basins (Maley & Maley, 1981, Ghienne *et al.*, 2002, Schuster *et al.*, 2005, Lemoalle *et al.*, 2012). The northern basin that forms the central lowlands of Chad, with the central depression of Bodélé (Moussa, 2010). It is bounded to the north and east by mountainous areas, respectively Tibesti and Ennedi, and to the southwest by the Late Pleistocene dune field of Kanem (Maley, 2000, Schuster *et al.*, 2005) To the south, the Chari-Logone basin (BCL), which is the focus of this work, is the hydrologically active part of the Lake Chad basin. It covers an area of 613 000 km<sup>2</sup>, and its banks are surrounded by a series of mountain ranges: Guera, Ouaddaï, Central African Massif and Adamaoua (Fig. 1).



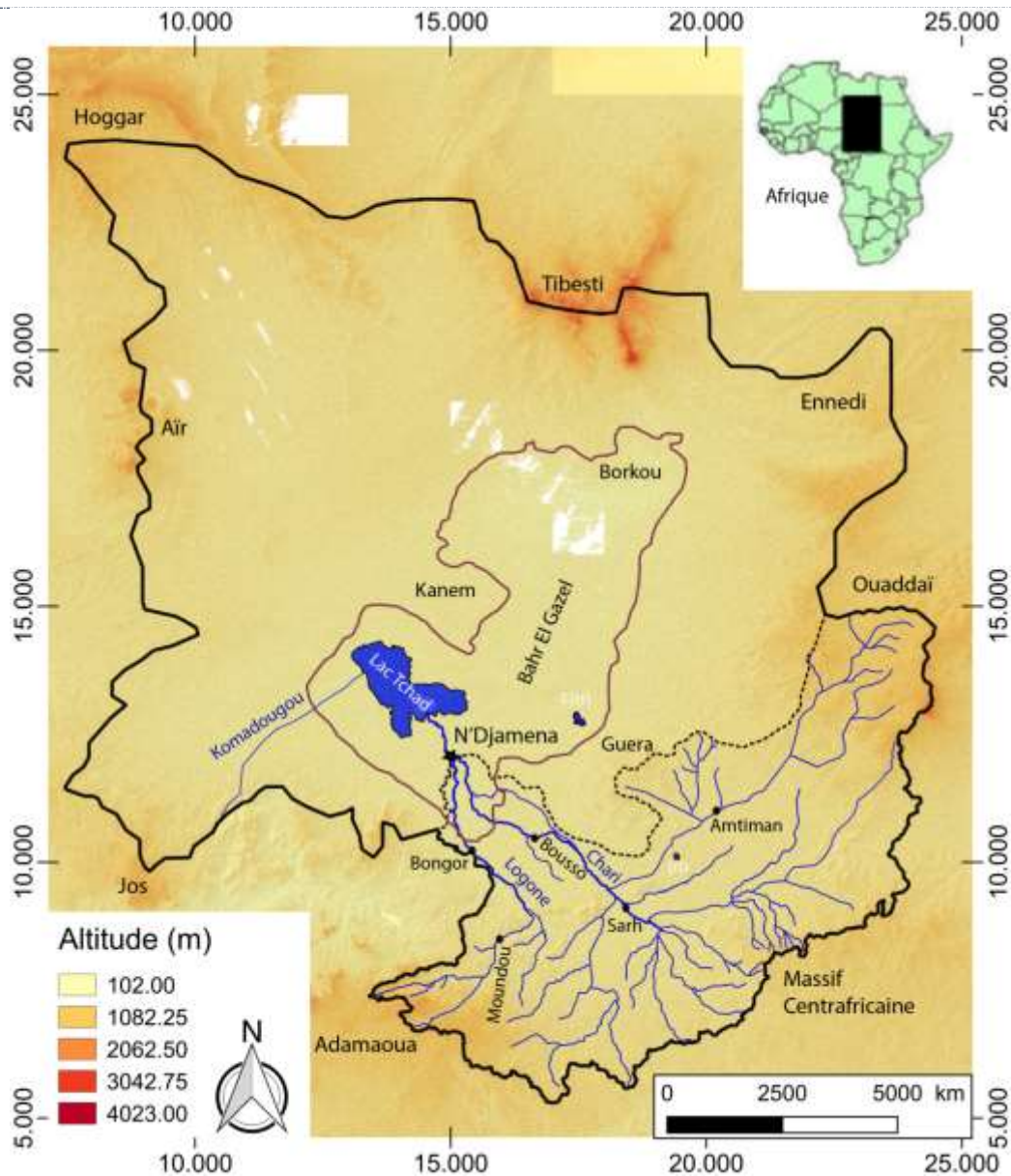


**Figure 1.** Map of the study area: the continuous black line marks the Lake Chad basin, the discontinuous black line that of the Chari-Logone basin and finally the brown line the Mega Lake Chad to the Holocene (Ghienne *et al.*, 2002, Schuster *et al.*, 2005, Leblanc *et al.*, 2006). Topo 30 Shuttle Radar Topography (SRTM) data, easily accessible and freely downloadable from the <https://earthexplorer.usgs.gov/> website

## 2.2 Description of the climate framework

The climatological data described here were provided by the General Directorate of National Meteorology of Chad (DGMN). The climate of the Chari-Logone basin is contrasted, from the tropical climate to the Sahelian climate. Climatic elements studied are temperature, rainfall, humidity and evaporation, monthly averages for the 1984-2014 period at the N'Djamena and Sarh stations (Fig.1). These stations may be representative of the tropical zone (Sarh) and the Sahelian zone (N'Djamena).

### 2.2.1 Temperatures

The average monthly heat regime shows two maxima: a peak in April, which is the warm season before the first rains, and a secondary peak in October, at the end of the rainy season (Fig. 2). The difference between the



monthly averages of temperatures shows minima of 24°C for N'Djamena and 25°C for Sarh (January) and maxima of 32°C for Sarh and 34°C for N'Djamena (April). Mean interannual temperatures are very variable.

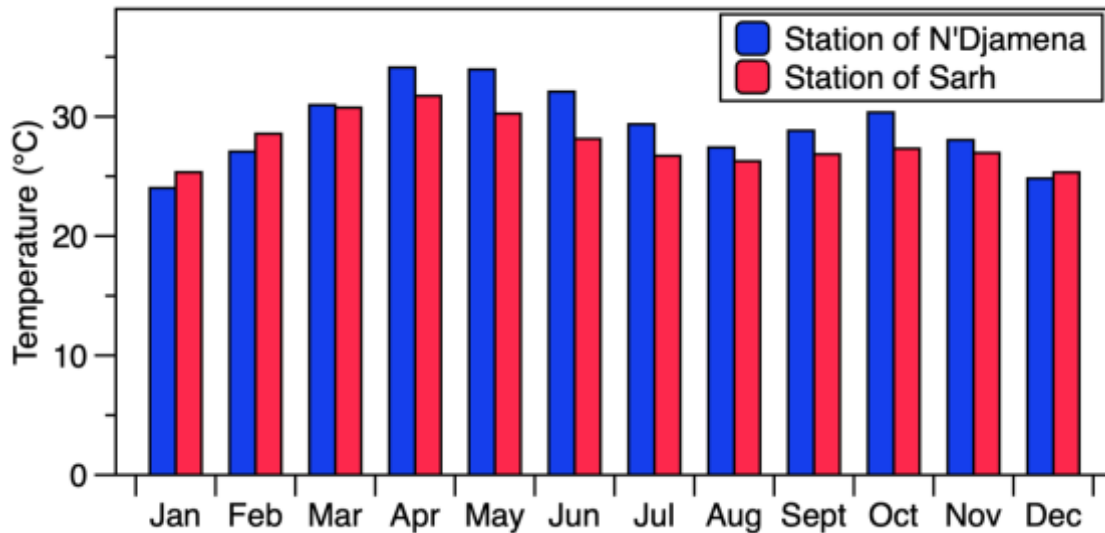


Figure 2: Average monthly temperature in N'Djamena and Sarh between 1984 and 2014

### 2.2.2 Precipitations

The analysis of the histogram of the monthly and interannual averages of the rainfall data of the two stations located in the Chari-Logone basin indicates that rainfall is decreasing from south to north. The southern station (Sarh) is the most watered, with an average annual rainfall of 972 mm, and that of N'Djamena is the least watered with an average rainfall of 544 mm. In the southern part of the basin, the rainy season starts earlier than in the North (April), and ends later (October); the difference being about a month. It is noted that the rains increase gradually to reach a maximum in August, before decreasing suddenly. The monthly evolution reveals an alternation of wet and dry periods. This change in rainfall during the year shows that the Chari-Logone basin has a tropical rainfall pattern at two seasons (Fig. 3): a wet season (April to October) and a dry season (November). to March). The duration of the rainy season is not the same everywhere. If it lasts four to six months in the southern part, it lasts only two to three months in the northern part of the basin. The rainiest months are those of July and August, which are at the heart of the rainy season.





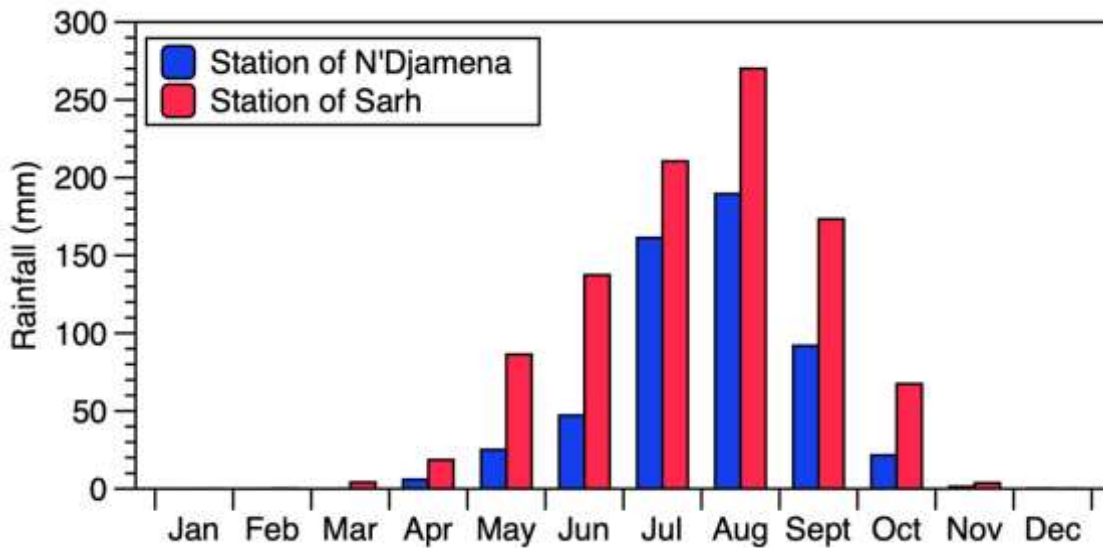


Figure 3 :Average monthly rainfall in N'Djamena and Sarh from 1984 to 2014

2.2.3 Humidity of the air

The relative humidity of the air follows a seasonal evolution identical to that of precipitations. The interannual monthly maximum is in August (Fig. 4) and is around 80% in Sarh and 85% in N'Djamena. The minimum, which is observed in February-March, varies from 23% for N'Djamena to 29% for Sarh. Air humidity varies with the frequency of winds in the area.

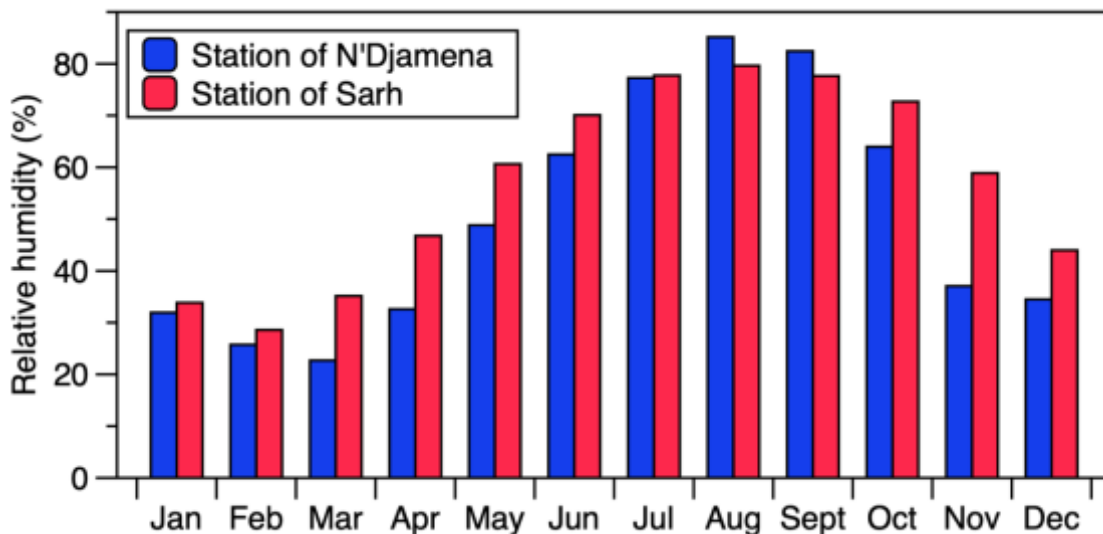


Figure 4: Average monthly relative humidity in N'Djamena and Sarh between 1984 and 2014

2.2.4 Evaporation

Measured with the Piche technique, evaporation varies almost in the same way as the air temperature and goes in the opposite direction of rainfall (Fig. 5). The seasonal cycle is well marked. The average monthly maximum evaporation is observed in March and reaches 281 and 416 mm in Sarh and N'Djamena respectively. The minimum is obtained in August, with 53 mm for Sarh and 77 mm for N'Djamena.

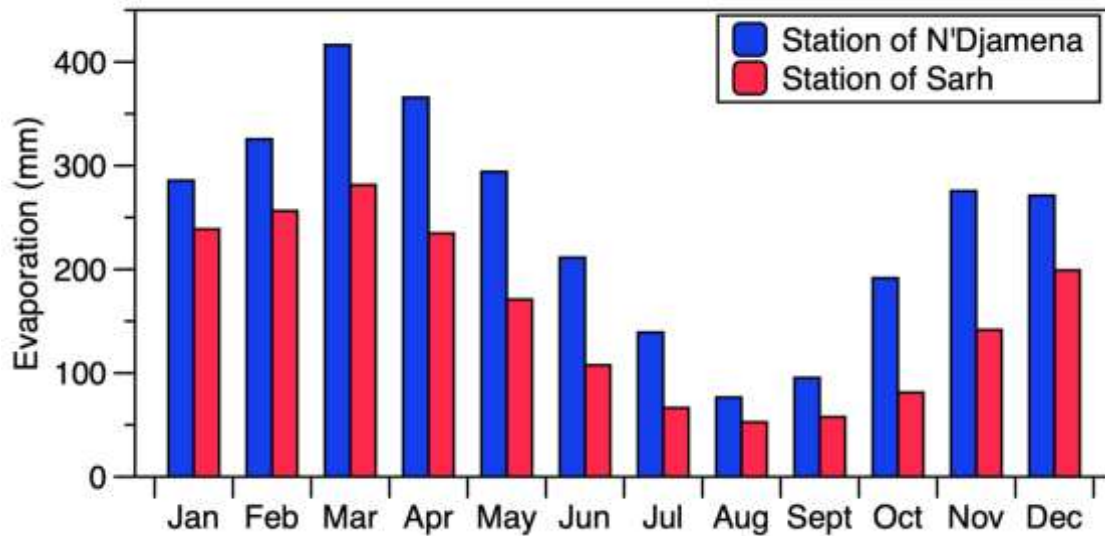


Figure 5 :Average monthly evaporation (Piche technique) in N'Djamena and Sarh between 1984 and 2014

### 2.3 Hydrography

The basin is drained by two main hydrographic networks, the Logone and the Chari rivers. The Logone river, with a length of 1000 km, originates in the Adamawa plateau in Cameroon, with an altitude ranging from 305 to 835 m (Cabot, 1965, Gac, 1980). The Chari Basin covers an area of approximately  $523 \cdot 10^3 \text{ km}^2$ . The convergence of the Chari and the Logone rivers is located in N'Djamena, 110 km upstream of Lake Chad, (Fig. 1). The total area of the Logone catchment is  $90 \cdot 10^3 \text{ km}^2$  at the confluence with the Chari. The Chari starts in the Central African Republic at an altitude between 500 and 600 m. It flows nearly 1200 km from the Central African Republic to the Lake Chad. The Chari-Logone receives water input from groundwaters of the Precambrian basement upper basin while in the lower part the Chari-Logone water flows from the river towards the Quaternary Aquifer (Bouchez *et al.*, 2019). The Chari-Logone baseflow discharge is supported by only 12% of the catchment (Bouchez *et al.* 2019).

## 3. RAINFALL DATA AVAILABLE

### 3.1 Rainfall data of national networks

The Chari-Logone basin is shared by four countries: Cameroon, Central Africa, Sudan and Chad. The acquisition and management of rainfall data on each national territory are managed by the competent services of each country.

In Chad, the General Directorate of National Meteorology (DGMN) of the Ministry of Civil Aviation and Meteorology has several meteorological stations in all the main cities or chief towns of the country's regions. Most of these stations were installed by researchers from the Office of Scientific and Technical Research Overseas (ORSTOM) and the Agency for the Safety of Air Navigation in Africa and Madagascar (ASECNA), during the colonial period. They are still most often functional despite a few interruptions linked in particular to the civil war experienced by Chad and the subregion in the late 1980s.

DGMN data is the only "real" data or measured directly in the field. The climate division of the DGMN provided us with the monthly data from 1960 to 2015 of 11 meteorological (rainfall) stations within and around the Chari-Logone basin (Fig. 6).

A systematic control of the quality of these data was performed on the raw data to ensure the reliability of the series. We have corrected and removed from the database the easily identifiable doubtful values due to typos or seizure of statements. This check only removed the obviously false values; but does not guarantee the accuracy/accuracy of the data stored.

We were unable to obtain data from the national networks of the Cameroonian, Central African and Sudanese parties.

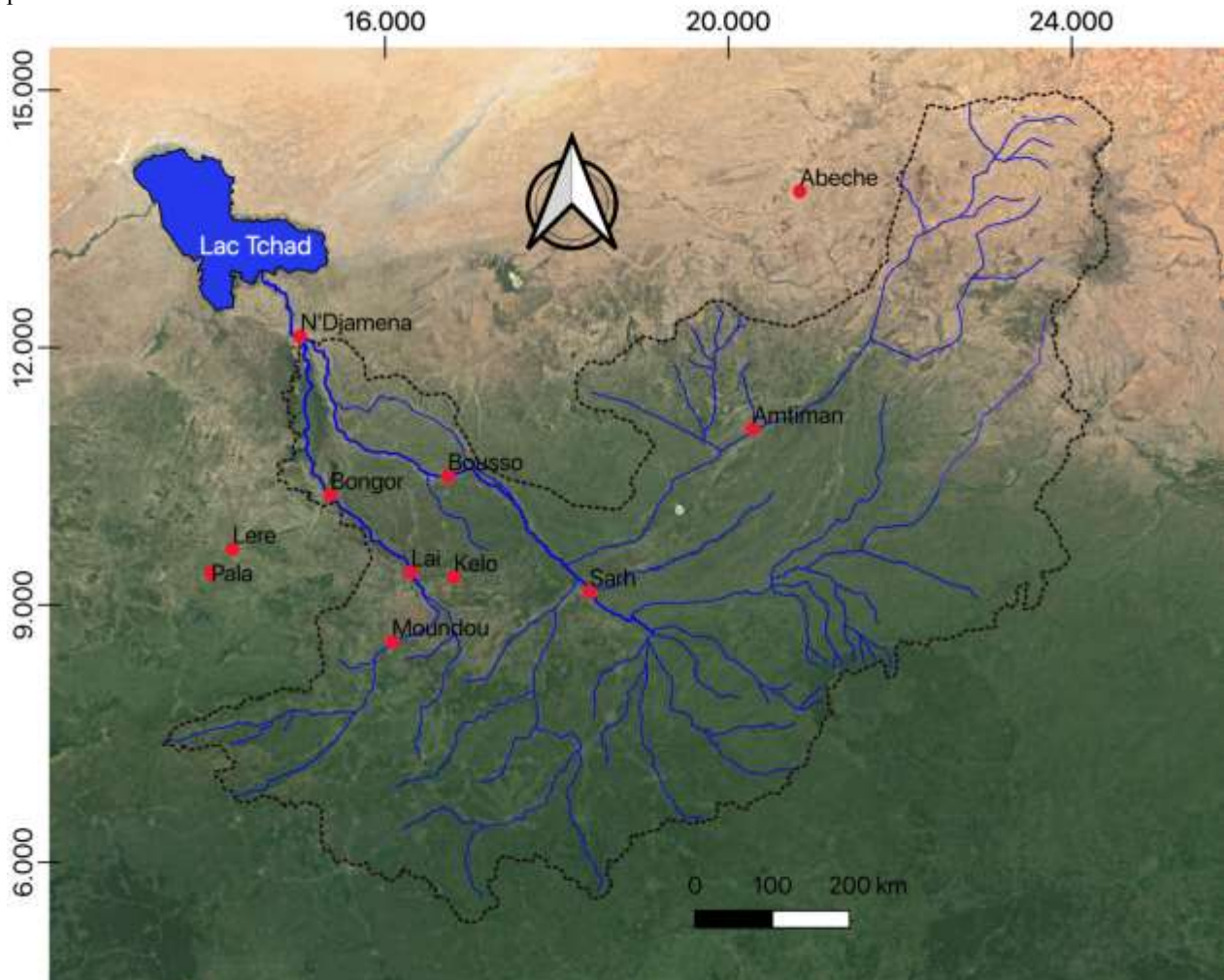


*Figure 6. Location of the eleven Chadian rainfall stations for which data are available at the monthly time step between 1960 and 2015 in the Chari-Logone basin (Source: DGMN). The black dashed line is the outline of the Chari-Logone basin.*

The station names, geographic coordinates, and interannual averages of the rainfall data obtained are shown in Table 1.



**Table 1: Characteristics of the eleven rainfall stations for which data are available at the monthly time step between 1960 and 2015 in the Chari-Logone basin (Source: DGMN).**

stations	Coordinates (projection: WGS 84)			Inter-annual average (mm)	STDEV
	Latitude	Longitude	Altitude (m)		
Abeché	13,82	20,83	545	351	109
Antiman	11,05	20,28	436	773	135
Bongor	10,28	15,37	328	786	172
Bouso	10,5	16,73	336	813	193
Kélo	9,32	16,8	378	1006	202
Laï	9,38	16,3	375	1004	173
Léré	9,65	14,22	265	875	144
Moundou	8,57	16,08	410	1078	154
N'Djamena	12,13	15,02	295	540	119
Pala	9,37	13,97	464	975	185
Sarh	9,15	18,38	365	990	159

### 3.2 Data from the literature

We have completed this database with rainfall data (monthly interannual averages) from two monographs carried out on the Chari and the Logone by ORSTOM:

- A monograph of Billon *et al.* (1968) on Chari using data from 74 stations distributed over the watershed, covering durations of 6 to 34 years over a selected period from 1940 to 1967;
- A monograph of Cabot (1965) on the Logone using data from 27 stations on the Logone, lasting from 4 to 27 years over a period from 1934 to 1956.

Altogether, the average data of 89 rainfall stations referenced are available in these two monographs (74 Chari monograph stations and 15 Logone monograph stations, these monographs having 12 common stations).

### 3.3 Data of CRU (Climate Research Unit)

The Climate Research Unit (CRU), University of East Anglia, Norwich, UK and the UK Department of Environment, Transport and Regions are providing a set of re-analyses of global climate data. These are calculated from a model and actual data, including monthly precipitation since 1900, at a resolution of 0.5° latitude and longitude. The method of treating precipitation in grids is described in the work of (Hulme *et al.*, 1995, Jones & Hulme, 1996). We used data from the CRU TS 4.02 version (<https://crudata.uea.ac.uk/cru/data/hrg/>) described by Harris *et al.* (2014). The monthly precipitation of the CRU has already been used in several studies in the Chari-Logone basin (Ardoin-Bardin *et al.*, 2009, Lemoalle *et al.*, 2012, Zhu *et al.*, 2019). These spatialized rainfall data were used as one of the input parameters of the rainfall-flow models.

## 4 METHODOLOGY

We present the process of spatialization of precipitation, then the method used to estimate the average precipitation for each of the sub-basins during the defined periods.

### 4.1 Estimate of precipitation by sub basins for 1960-2015

Data from the Billon *et al.* (1968) and Cabot (1965) monographs covering the period 1940-1960 were used to determine the spatial distribution of mean annual rainfall. There is no longer a data set covering a more recent period with sufficient spatial coverage to perform a satisfactory spatial interpolation. The average precipitation per sub-basin is determined from the interpolated map (cf result). It is then assumed that the spatial distribution

is stable over time, and mean precipitation per sub-basin is considered to vary jointly. The time series of the available stations are then used to characterize the precipitation variations.

#### 4.2 Spatialization of precipitation

We describe in the lines that follow the method of obtaining spatialized rainfall over the Chari-Logone basin. An interpolation by kriging is carried out from annual average rainfall.

##### 4.2.1 Data used for the spatialization of precipitation

Monographs on Chari (Billon *et al.*, 1968) and Logone (Cabot, 1965) have pluviometry data distributed over the four countries that cover the Chari-Logone basin with good spatial coverage (Fig. 7).

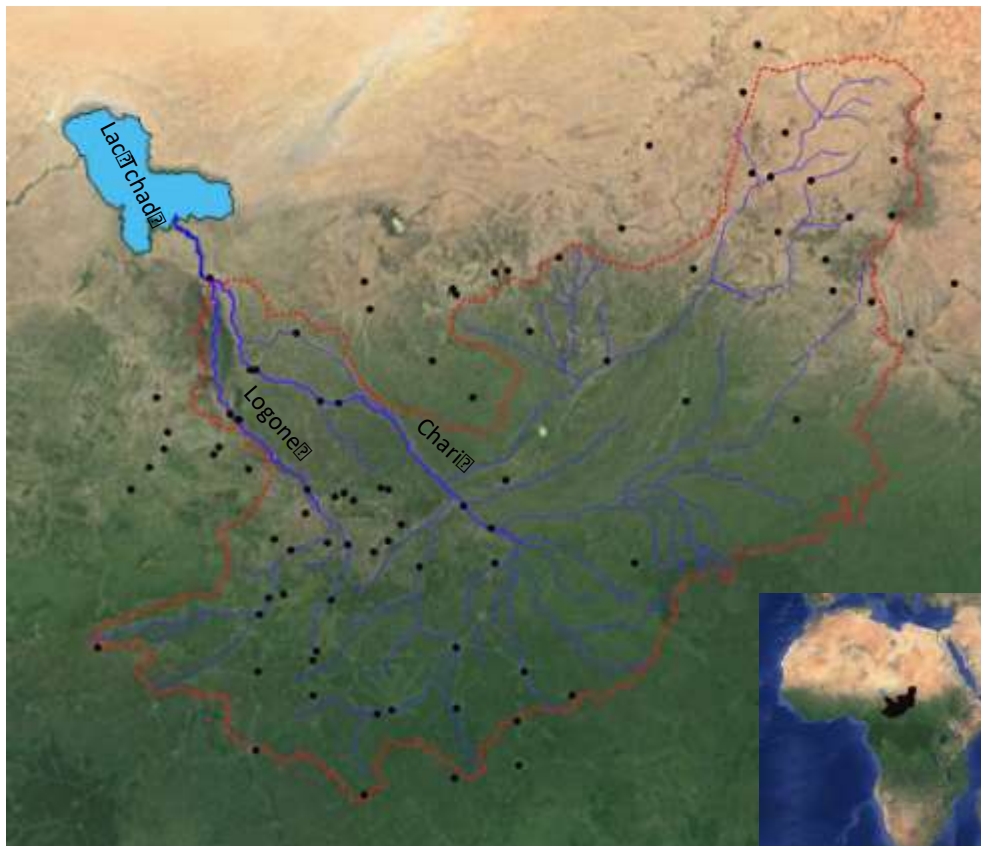


Figure 7 :Location (black dots) of rainfall stations from the two monographs of Chari (Billon *et al.*, 1974) and Logone (Cabot, 1965). The red line is the outline of the Chari-Logone basin.

##### 4.2.2 Kriging interpolation method

Kriging is a process by which a quantity, here precipitation, is interpolated from a randomly distributed set of data (x, y, z). It is based on the average of a local estimate in which each estimate is a weighted average of the values observed in the neighborhood. The result of the interpolation provides a structured data called "grid".

Widely used (Woodley *et al.*, 1979, Chong *et al.*, 1987), the kriging interpolation method makes it possible to characterize the distribution and variability of rain fields and to quantify the estimation error of the surface averages. Its advantage is to provide both the best estimate of rainfall at all points and the uncertainty associated with the estimate. This method is based on the Regionalized Variables Theory. This theory comes from the Theory of Random Functions (Matheron, 1966), used to solve data estimation problems by taking into account the spatial structure of the variables to be treated.

The semi-variogram is commonly used to analyze the inter-distance dependence of spatial observations (Ruelle *et al.*, 1986). It makes it possible to determine whether the distribution of the parameter (s) studied is regionalized, random or periodic. A variogram is characterized by the following parameters: nugget, span and bearing (Fig. 8). It is necessary to draw and study the variogram because its appearance makes it possible to highlight three main characteristics (Smith *et al.*, 1993):

- Nugget effect: Very short-lived variation, location errors, analysis errors and analytical precision. It can be induced either by measurement errors assumed to be random and not regionalised, or by the existence of a spatial variability defined over a smaller distance than the smallest distance class taken into account in the variogram.
- Scope: Distance where two observations are no longer alike at all on average and are no longer linked (linear covariance) linearly. At this distance, the value of the variogram corresponds to the variance of the random variable. Scope is used to set the optimal sampling interval since samples taken at a distance less than the range are spatially dependent (Ruelle *et al.*, 1986). We see that when the range is reached, there is no more covariance between the random variables.
- Bearing: The bearing is characterized by reaching a plateau where the semi-variance of the data becomes constant with the evolution of inter-sample distance. To relocate under the conditions of the intrinsic hypothesis, it is then necessary to filter the relation between the random function and the x-coordinates computed by linear or quadratic regressions. The analysis of the structure can be taken from the drift residues thus calculated (Goovaerts, 2000, Snepvangers *et al.*, 2003).

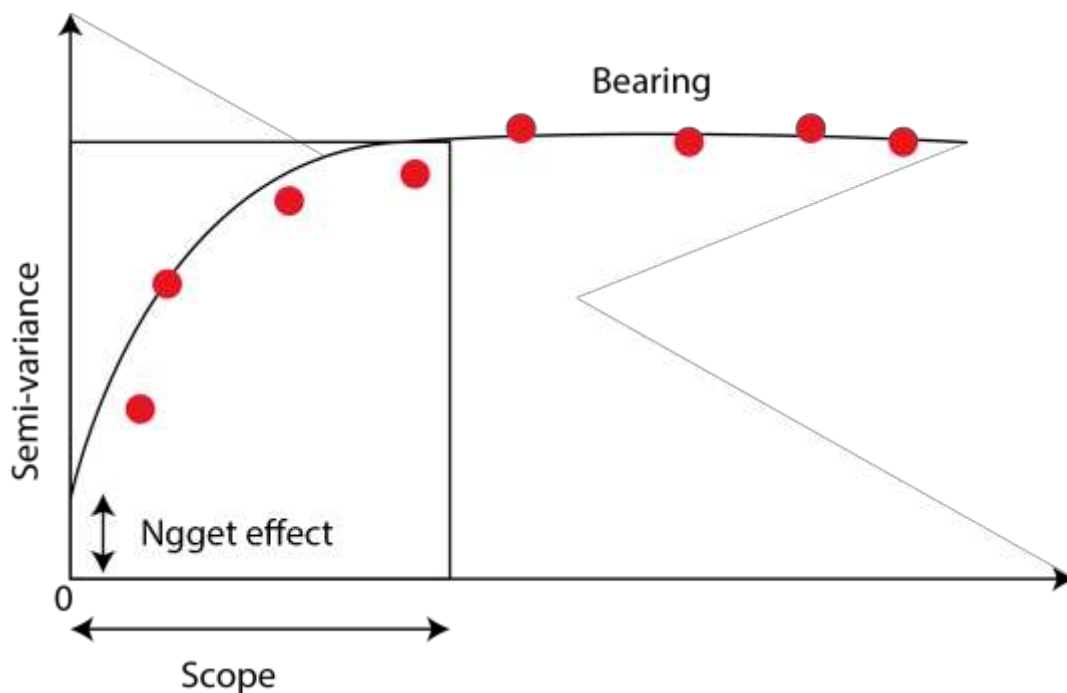


Figure 8. Theoretical semi-variogram (spherical model)

The kriging interpolation of the rainfall data from the rainfall measuring stations is performed using the "R" software. The libraries (packages) used are : gstat, sp, rcpp, plyr, reshape, automap, circular, MASS, geoR, Metrics, rgdal, lattice, maptools, raster et latticeExtra.

#### 4.2.3 Average Spatial Precipitation of the Chari-Logone Basin

The steps used for long-term spatio-temporal precipitation reconstruction are:

- the mean spatial rainfall of the basin  $i$  ( $P_i$ , monog) is determined for the period 1940-1960 from the krigated map;
-

- then, assuming that this spatial distribution is always the same, the temporal variations are determined from the 11 precipitation stations which, included in the stations used for kriging, also cover the period 1960-2015 (DGMN). The average precipitation of a year "a" is compared to the period 1940-1960 from a coefficient  $ka$  defined as follows:

$$ka = \frac{P_a}{P_{MONOG}}$$

Where  $P_a$  is the average of the 11 annual precipitation values for year a, and  $P_{MONOG}$  is the average of the 11 inter-annual precipitation values for the 1940-1960 period from the Chari and Logone monographs.

- Spatial rainfall for each sub-basin  $i$  and for each year  $a$  is then calculated as follows:

$$P_{i,a} = ka * P_{i,monog}$$

Thus we reconstructed the annual average rainfall of Chari Logone from 1960 to 2015.

## 5 RESULTS AND DISCUSSIONS

### 5.1 Interpolation by precipitation kriging

#### 5.1.1 Semi variogram

Semi variograms constructed with raw data have no level of variance (Fig. 9). When no level is identifiable, it is recommended to work on the residuals (Goovaerts, 2000, Snepvangers *et al.*, 2003), which represent the difference between the variable and a surface, for example a plan determined by the adjustment of the data considered by the least squares method (Séraphin, 2016). Thus, this method makes it possible to subtract the linear trends from the rainfall data resulting from the latitudinal or continental effects, to interpret only the local variations of the pluviometry.

For the analysis of the anisotropy of the rainfall distribution, we established the directional variograms (Fig. 9) in four directions ( $0^\circ$ ,  $45^\circ$ ,  $90^\circ$  and  $135^\circ$ ).

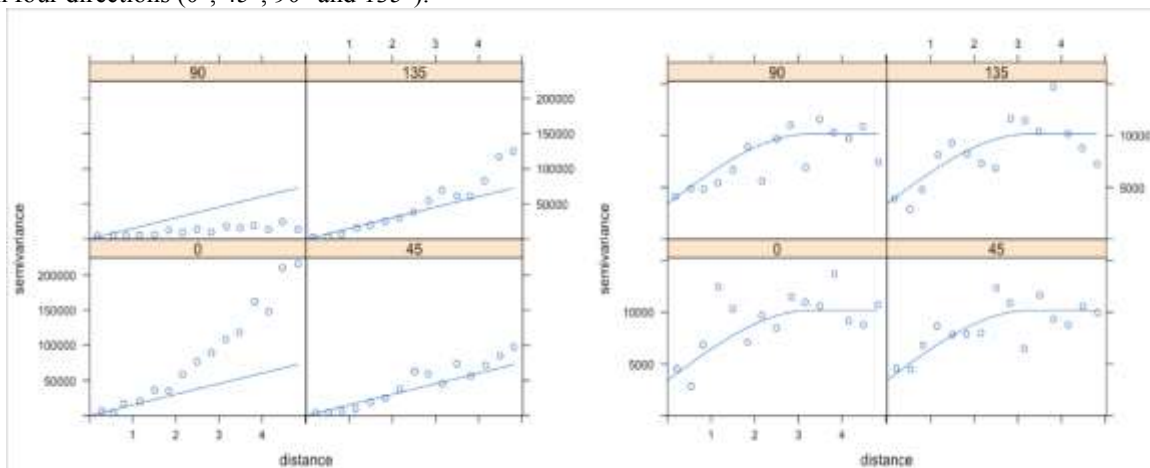


**Figure 9: Semi variograms of the raw data (figure on the left) and the residuals (figure its lines) in the four directions (0, 45, 90 and 135 °) made with a spherical model**

Examination of the variographic surface of the residues obtained from the rainfall data shows a plateau (Fig. 9) thus making it possible to adjust conventional variographic models. The models and parameters used are shown in Table 2.

*Table 2: Calibration Parameters and Semi Variogram Models*

Parameter	Characteristics
Model	Spherical
Seuil	7800
scope	3
Nugget effect	3500
Variance	10550.15

### 5.1.2 Average rainfall over the Chari-Logone basin

The interpolation is made on eighty-nine rainfall stations, and the mesh chosen is a regular grid with a pitch of  $0.1^\circ$ . The analysis in Figure 10 shows that the distribution of mean interannual rainfall is mainly along a south-north gradient typical of the Sudano-Sahelian region. The highest values are always recorded at the southwestern extremities corresponding to the direction of entry of the monsoon flow in the basin, with probably a slight orographic effect. Thus, Sudan's wetter regions of the south-west (1600 to 800 mm) are progressively transferred to the Sahelian regions, which are sparsely watered in the north-east (between 800 and 200 mm).

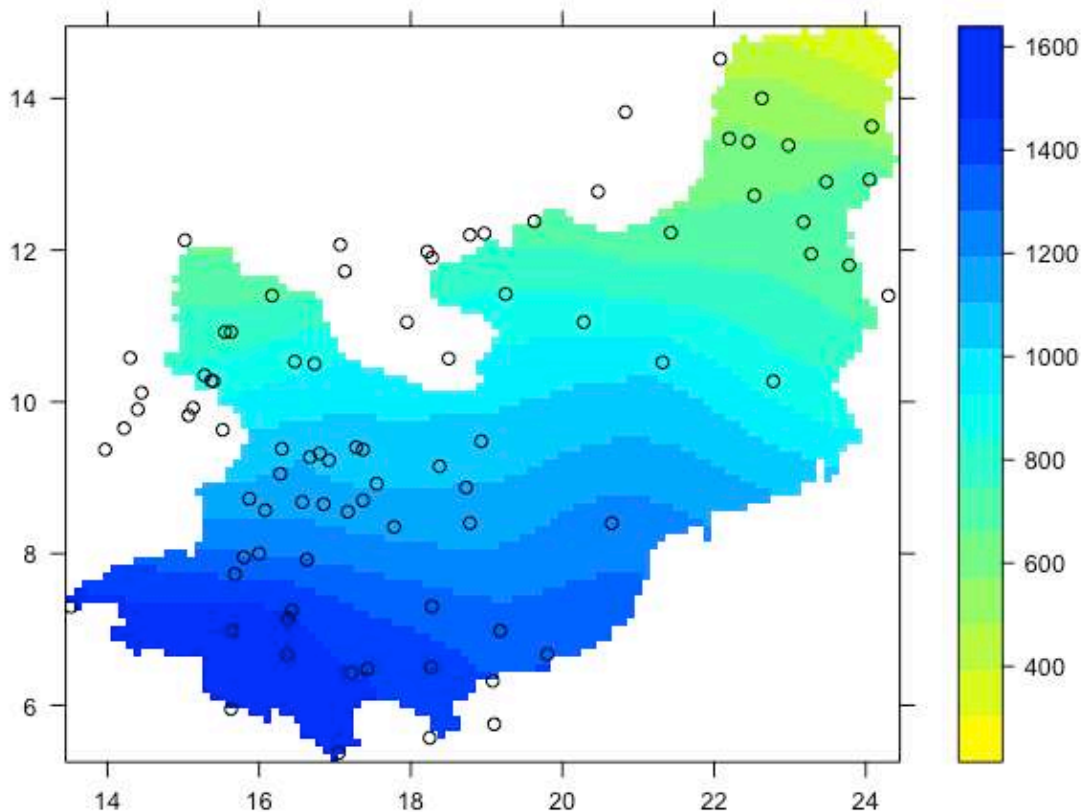


*Figure 10: Spatial distribution of average rainfall for the period 1940-1960 in the Chari-Logone basin and location of the 89 rainfall stations used (Data taken from the Chari monographs (Cabot, 1965) and Logone Billon et al (1968))*

### 5.2 Comparison with CRU data

The spatio-temporal precipitation obtained for this work and that of the CRU are relatively comparable (Fig. 11), except from the 1950s for which precipitation data are rarer. This scarcity after 1980 leads to significant uncertainties in the estimation of spatialized rainfall, both with CRU data and from the method applied in this work.



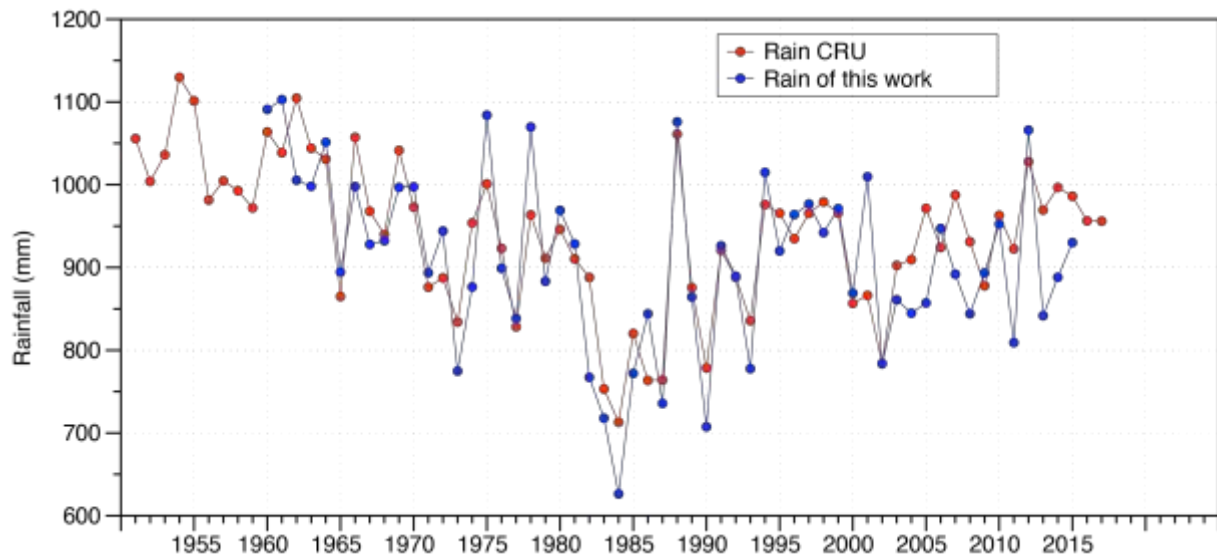


Figure 11. Comparison of spatialized rainfall over the Chari-Logone basin obtained by the CRU and this study

## 6 SUMMARY AND CONCLUSIONS

The Chari-Logone basin is tributary to the Atlantic Ocean, which is subject to a climate induced by the seasonal movement of two air masses separated by a front (Olivry, 2002). The front or the Intertropical Convergence Zone (ITCZ) is the site of a confluence between two air masses: on the one hand, the monsoon, humid, of oceanic origin, of southwest sector; and Harmattan, dry, northeastern and continental in origin (S. E. Nicholson, 2015). This movement of the ITCZ leads to the seasonal variability of the rainfall regime in the Chari-Logone basin. The latter recorded two well-marked seasons in the year: a short rainy season centered on the summer (June-September) and a long dry season centered on the winter.

During the dry season, from November to March, the ITCZ is found around  $5^{\circ}$  -  $7^{\circ}$  N (Lienou, 2007) where there is a predominance of Harmattan (Leroux, 1986). From April, a slight rise in the ITCZ gives rise to rainfall in the southern part of the Chari-Logone basin. Then the ITCZ goes back to the northernmost part in July-August, the wettest months of the year. As of September-October, the ITCZ is rapidly moving southward (S. Nicholson, 2000). The dry season sets in at the beginning of October in the northern part of the country while in the south, rains can be recorded until November.

In addition, factors controlling the temporal variability of precipitation must be large-scale aspects of the general atmospheric circulation, such as Walker or Hadley circulation or monsoon intensities, or oceanic influences, such as surface temperatures from the sea (Nicholson, 2000). The contrast between dry and wet years is associated with a weakening and contraction of the tropical rain belt (S. E. Nicholson, 2008, 2009). Sea surface temperatures play a key role in the location of the ITCZ (Giannini *et al.*, 2003)

## 7 ACKNOWLEDGEMENTS

This work was supported by the French National Research Institute for Sustainable Development (IRD) in the framework of the project 'Préservation du Lac Tchad: Contribution à la stratégie de développement du lac' funded by 'Fond Français de l'Environnement Mondial' and by 'Agence Française pour le Développement'. The authors are grateful to the University of N'Djamena, the Centre National de la Recherche pour le Développement of Chad (CNRD) and the French Embassy in Chad for their logistical support.

## REFERENCES

- [1] Ardoin-Bardin, S., Dezetter, A., Servat, E., Paturel, J. E., Mahé, G., Niel, H. & Dieulin, C. (2009) Using general circulation model outputs to assess impacts of climate change on runoff for large hydrological catchments in West Africa. *Hydrol. Sci. J.*54(1), 77–89. doi:10.1623/hysj.54.1.77
- [2] Baillargeon, S. (2005) Le krigeage : revue de la théorie et application à l'interpolation spatiale de données de précipitations. Retrieved from <https://corpus.ulaval.ca/jspui/handle/20.500.11794/18036>
- [3] Billon, B., Guiscafré, J., Herbaud, J. & Oberlin, G. (1968) Monographie hydrologique du Chari, 145 + 289 + 99 + 235 + 477 p. multigr. Paris: ORSTOM. Retrieved from <http://www.documentation.ird.fr/hor/fdi:16679>
- [4] Bouchez, C., Deschamps, P., Goncalves, J., Hamelin, B., Mahamat Nour, A., Vallet-Coulomb, C. & Sylvestre, F. (2019) Water transit time and active recharge in the Sahel inferred by bomb-produced <sup>36</sup>Cl. *Sci. Rep.*9(1), 7465. doi:10.1038/s41598-019-43514-x
- [5] Cabot, J. (1965) Le bassin du moyen Logone. Mémoires ORSTOM, 328 p. Paris: ORSTOM. Retrieved from <http://www.documentation.ird.fr/hor/fdi:10420>
- [6] Chevallier, P. & Pouyaud, B. (1996) La distribution spatio-temporelle des pluies au Sahel: Apport de l'expérience EPSAT Niger. IAHS. Retrieved from [https://books.google.fr/books?hl=fr&lr=&id=azUCAebIN-YC&oi=fnd&pg=PA77&dq=La+distribution+spatio-temporelle+des+pluies+au+Sahel:+Apport+de+l%2E%80%99experience+EPSAT+&ots=MWSiynl-Av&sig=XapD1HSRaNh-JEqIXwDtq5Zob\\_Y#v=onepage&q=La%20distribution%20spatio-temporelle%20des%20pluies%20au%20Sahel%3A%20Apport%20de%20l%2E%80%99experience%20EPSAT&f=false](https://books.google.fr/books?hl=fr&lr=&id=azUCAebIN-YC&oi=fnd&pg=PA77&dq=La+distribution+spatio-temporelle+des+pluies+au+Sahel:+Apport+de+l%2E%80%99experience+EPSAT+&ots=MWSiynl-Av&sig=XapD1HSRaNh-JEqIXwDtq5Zob_Y#v=onepage&q=La%20distribution%20spatio-temporelle%20des%20pluies%20au%20Sahel%3A%20Apport%20de%20l%2E%80%99experience%20EPSAT&f=false)
- [7] Chong, M., Amayenc, P., Scialom, G. & Testud, J. (1987) A Tropical Squall Line Observed during the COPT 81 Experiment in West Africa. Part 1: Kinematic Structure Inferred from Dual-Doppler Radar Data. *Mon. Weather Rev.*115(3), 670–694. doi:10.1175/1520-0493(1987)115<0670:ATSLOD>2.0.CO;2
- [8] Dingman, S. L., Seely-Reynolds, D. M. & Reynolds, R. C. (1988) Application of Kriging to Estimating Mean Annual Precipitation in a Region of Orographic Influence. *JAWRA J. Am. Water Resour. Assoc.*24(2), 329–339. doi:10.1111/j.1752-1688.1988.tb02991.x
- [9] Funk, C., Verdin, A., Michaelsen, J., Peterson, P., Pedreros, D. & Husak, G. (2015) A global satellite assisted precipitation climatology. doi:10.5194/essd-7-275-2015
- [10] Gac, J.-Y. (1980) Géochimie du bassin du lac Tchad : Bilan de l'altération de l'érosion et de la sédimentation. ORSTOM, Paris. Retrieved from <http://www.documentation.ird.fr/hor/fdi:00039>
- [11] Ghienne, J.-F., Schuster, M., Bernard, A., Düringer, P. & Brunet, M. (2002) The Holocene giant Lake Chad revealed by digital elevation models. *Quat. Int.*87(1), 81–85. doi:10.1016/S1040-6182(01)00063-5
- [12] Giannini, A., Saravanan, R. & Chang, P. (2003) Oceanic Forcing of Sahel Rainfall on Interannual to Interdecadal Time Scales. *Science*302(5647), 1027–1030. doi:10.1126/science.1089357
- [13] Goovaerts, P. (2000) Geostatistical approaches for incorporating elevation into the spatial interpolation of rainfall. *J. Hydrol.*228(1), 113–129. doi:10.1016/S0022-1694(00)00144-X
- [14] Houghton, J. T. (1992) Climate Change 1992. Retrieved from <http://adsabs.harvard.edu/abs/1992clch.book.....H>
- [15] Huffman, G. J., Adler, R. F., Rudolf, B., Schneider, U. & Keehn, P. R. (1995) Global Precipitation Estimates Based on a Technique for Combining Satellite-Based Estimates, Rain Gauge Analysis, and NWP Model Precipitation Information. *J. Clim.*8(5), 1284–1295. doi:10.1175/1520-0442(1995)008<1284:GPEBOA>2.0.CO;2
- [16] Hulme, M., Conway, D., Jones, P. D., Jiang, T., Barrow, E. M. & Turney, C. (1995) Construction of a 1961–1990 European climatology for climate change modelling and impact applications. *Int. J. Climatol.*15(12), 1333–1363. doi:10.1002/joc.3370151204
- [17] Jones, P. D. & Hulme, M. (1996) Calculating Regional Climatic Time Series for Temperature and Precipitation: Methods and Illustrations. *Int. J. Climatol.*16(4), 361–377. doi:10.1002/(SICI)1097-0088(199604)16:4<361::AID-JOC53>3.0.CO;2-F

- [18] Joyce, R. & Arkin, P. A. (1997) Improved Estimates of Tropical and Subtropical Precipitation Using the GOES Precipitation Index. *J. Atmospheric Ocean. Technol.*14(5), 997–1011. doi:10.1175/1520-0426(1997)014<0997:IEOTAS>2.0.CO;2
- [19] L. D. Meyer. (1981) How Rain Intensity Affects Interrill Erosion. *Trans. ASAE*24(6), 1472–1475. doi:10.13031/2013.34475
- [20] Leblanc, M., Favreau, G., Maley, J., Nazoumou, Y., Leduc, C., Stagnitti, F., Oevelen, P. J. van, et al. (2006) Reconstruction of Megalake Chad using Shuttle Radar Topographic Mission data. *Palaeogeogr. Palaeoclimatol. Palaeoecol.*239(1–2), 16–27. doi:10.1016/j.palaeo.2006.01.003
- [21] Lemoalle, J., Bader, J.-C., Leblanc, M. & Sedick, A. (2012) Recent changes in Lake Chad: Observations, simulations and management options (1973–2011). *Glob. Planet. Change*80–81, 247–254. doi:10.1016/j.gloplacha.2011.07.004
- [22] Leroux, M. (1986) L'Anticyclone mobile Polaire : facteur premier de la climatologie tempérée (The Polar mobile Anticyclone : first factor of temperate climatology). *Bull. Assoc. Géographes Fr.*63(4), 311–328. doi:10.3406/bagf.1986.1354
- [23] Lienou, G. (2007) Impacts de la variabilité climatique sur les ressources en eau et les transports de matières en suspension de quelques bassins versants représentatifs au Cameroun. These Dr. PhD Univ. Yaoundé I. Retrieved from <https://core.ac.uk/download/pdf/39839507.pdf>
- [24] Maley, J. (2000) Last Glacial Maximum lacustrine and fluvial Formations in the Tibesti and other Saharan mountains, and large-scale climatic teleconnections linked to the activity of the Subtropical Jet Stream. *Glob. Planet. Change Paleomonsoon variations and terrestrial environmental change* 26(1), 121–136. doi:10.1016/S0921-8181(00)00039-4
- [25] Maley, J. & Maley, J. (1981) Etudes palynologiques dans le bassin du Tchad et paléoclimatologie de l'Afrique nord-tropicale de 30 000 ans à l'époque actuelle. Retrieved from [https://www.researchgate.net/profile/Jean\\_Maley2/publication/37890068\\_Etudes\\_palynologiques\\_dans\\_le\\_bassin\\_du\\_Tchad\\_et\\_paleoclimatologie\\_de\\_l'Afrique\\_nord-tropicale\\_de\\_30\\_000\\_ans\\_a\\_l'epoque\\_actuelle/links/0a85e53a99756c7d61000000/Etudes-palynologiques-dans-le-bassin-du-Tchad-et-paleoclimatologie-de-l'Afrique-nord-tropicale-de-30-000-ans-a-lepoque-actuelle.pdf](https://www.researchgate.net/profile/Jean_Maley2/publication/37890068_Etudes_palynologiques_dans_le_bassin_du_Tchad_et_paleoclimatologie_de_l'Afrique_nord-tropicale_de_30_000_ans_a_l'epoque_actuelle/links/0a85e53a99756c7d61000000/Etudes-palynologiques-dans-le-bassin-du-Tchad-et-paleoclimatologie-de-l'Afrique-nord-tropicale-de-30-000-ans-a-lepoque-actuelle.pdf)
- [26] Matheron, G. (1966) Présentation des variables régionalisées. *J. Société Fr. Stat.*107, 263–275. Retrieved from [http://www.numdam.org/article/JSFS\\_1966\\_\\_107\\_\\_263\\_0.pdf](http://www.numdam.org/article/JSFS_1966__107__263_0.pdf)
- [27] Moussa, A. (2010, January 1) Les séries sédimentaires fluviales, lacustres et éoliennes du bassin du Tchad depuis le Miocène terminal (thesis). Strasbourg. Retrieved from <http://www.theses.fr/2010STRA6185>
- [28] Nicholson, S. (2000) Land surface processes and Sahel climate. *Rev. Geophys.*38(1), 117–139. doi:10.1029/1999RG900014
- [29] Nicholson, S. E. (2001) Climatic and environmental change in Africa during the last two centuries. *Clim. Res.*17(2), 123–144. doi:10.3354/cr017123
- [30] Nicholson, S. E. (2008) The intensity, location and structure of the tropical rainbelt over west Africa as factors in interannual variability. *Int. J. Climatol.*28(13), 1775–1785. doi:10.1002/joc.1507
- [31] Nicholson, S. E. (2009) A revised picture of the structure of the “monsoon” and land ITCZ over West Africa. *Clim. Dyn.*32(7), 1155–1171. doi:10.1007/s00382-008-0514-3
- [32] Nicholson, S. E. (2015) Evolution and current state of our understanding of the role played in the climate system by land surface processes in semi-arid regions. *Glob. Planet. Change*133, 201–222. doi:10.1016/j.gloplacha.2015.08.010
- [33] Olivry, J.-C. (2002) Synthèse des connaissances hydrologiques et potentiel en ressources en eau du fleuve Niger. World Bank Niger Basin Auth. Provisional Rep.160. Retrieved from <http://www.hydrologie.org/BIB/Olivry-Niger/Niger.pdf>
- [34] Rozante, J. R., Moreira, D. S., Goncalves, L. G. de & Vila, D. A. (2010) Combining TRMM and Surface Observations of Precipitation: Technique and Validation over South America. *Weather Forecast.*25(3), 885–894. doi:10.1175/2010WAF2222325.1
- [35] Ruelle, P., Ben Salah, D. & Vauclin, M. (1986) Méthodologie d'analyse de la variabilité spatiale d'une parcelle agricole. Application à l'échantillonnage. *Agronomie*6(6), 529–539. doi:10.1051/agro:19860605

- [36] Schuster, M., Roquin, C., Durringer, P., Brunet, M., Caugy, M., Fontugne, M., Taïssou Mackaye, H., et al. (2005) Holocene Lake Mega-Chad palaeoshorelines from space. *Quat. Sci. Rev.*24(16), 1821–1827. doi:10.1016/j.quascirev.2005.02.001
- [37] Séraphin, P. (2016, November 23) Contribution du traçage isotopique ( $\delta$  18O et  $\delta$  D) à la compréhension et à la modélisation hydrogéologique de la nappe de la Crau (thesis). Aix-Marseille. Retrieved from <http://www.theses.fr/2016AIXM4353>
- [38] Smith, J. L., Halvorson, J. J. & Papendick, R. I. (1993) Using multiple-variable indicator kriging for evaluating soil quality. *Soil Sci. Soc. Am. J. USA*. Retrieved from <http://agris.fao.org/agris-search/search.do?recordID=US9430084>
- [39] Snepvangers, J. J. C., Heuvelink, G. B. M. & Huisman, J. A. (2003) Soil water content interpolation using spatio-temporal kriging with external drift. *Geoderma Pedometrics* 2001 112(3), 253–271. doi:10.1016/S0016-7061(02)00310-5
- [40] Subyani, A. M. (2004) Geostatistical study of annual and seasonal mean rainfall patterns in southwest Saudi Arabia / Distribution géostatistique de la pluie moyenne annuelle et saisonnière dans le Sud-Ouest de l'Arabie Saoudite. *Hydrol. Sci. J.*49(5), null-817. doi:10.1623/hysj.49.5.803.55137
- [41] Verdin, A., Funk, C., Rajagopalan, B. & Kleiber, W. (2016) Kriging and Local Polynomial Methods for Blending Satellite-Derived and Gauge Precipitation Estimates to Support Hydrologic Early Warning Systems. *IEEE Trans. Geosci. Remote Sens.*54(5), 2552–2562. doi:10.1109/TGRS.2015.2502956
- [42] Woodley, W. L., Griffith, C. G., Griffin, J. S. & Stromatt, S. C. (1979) The Inference of GATE Convective Rainfall from SMS-1 Imagery. *J. Appl. Meteorol.*19(4), 388–408. doi:10.1175/1520-0450(1980)019<0388:TIOGCR>2.0.CO;2
- [43] Xie, P. & Arkin, P. A. (1997) Global Precipitation: A 17-Year Monthly Analysis Based on Gauge Observations, Satellite Estimates, and Numerical Model Outputs. *Bull. Am. Meteorol. Soc.*78(11), 2539–2558. doi:10.1175/1520-0477(1997)078<2539:GPAYMA>2.0.CO;2
- [44] Zhu, W., Jia, S., Lall, U., Cao, Q. & Rashid, M. (2019) Relative contribution of climate variability and human activities on the T water loss of the Chari/Logone River discharge into Lake Chad: A conceptual and statistical approach - Recherche Google 569, 519–531. doi:10.1016/j.jhydrol.2018.12.015.